THE JOURNAL OF PHYSICAL CHEMISTRY B

Article

pubs.acs.org/JPCB

Conformation and Dynamics of a Cyclic Disulfide-Bridged Peptide: Effects of Temperature and Solvent

Fee Li,[†] Kenny Bravo-Rodriguez,[‡] Charlotte Phillips,[§] Rüdiger W. Seidel,[∥] Florian Wieberneit,[⊥] Raphael Stoll,[⊥] Nikos L. Doltsinis,[§,#] Elsa Sanchez-Garcia,*[,‡] and Wolfram Sander*[,†]

[†]Lehrstuhl für Organische Chemie II, Ruhr-Universität Bochum, Universitätsstrasse 150, 44801 Bochum, Germany

[‡]Theoretische Chemie, Max-Planck-Institut für Kohlenforschung, Kaiser-Wilhelm-Platz 1, 45470 Mülheim an der Ruhr, Germany

[§]Department of Physics, King's College London, WC2R 2LS, London, United Kingdom

[∥]Lehrstuhl für Analytische Chemie, Ruhr-Universität Bochum, Universitätsstrasse 150, 44801 Bochum, Germany

[⊥]Biomolecular NMR, Ruhr-Universität Bochum, Universitätsstrasse 150, 44801 Bochum, Germany

[#]Institut für Festkörpertheorie, Universität Münster, Wilhelm-Klemm-Strasse 10, 48149 Münster, Germany

Supporting Information

ABSTRACT: The cyclic disulfide-bridged tetrapeptide cyclo-(Boc-Cys-Pro-Gly-Cys-OMe) (**1**) was designed as a model for the study of solvent-driven conformational changes in peptides. The three-dimensional structure and dynamics of **1** were studied using a variety of experimental and computational techniques. The crystal structure of **1** reveals a β-turn stabilized by a hydrogen bond between the two cysteine residues. In solution, the UV−CD and NMR analysis of **1** suggest a β-turn II conformation, stable up to 60 °C. The characteristic NMR ^{13}C shifts of the C_β and C_γ atoms of proline show that the peptide adopts exclusively the energetically favored trans conformation of the peptidyl-prolyl bond. The combination of IR spectroscopy with Car−Parrinello MD simulations and DFT calculations allowed us to assign the absorptions in the amide I region to the individual amino acids. The NH group of Gly, which as hydrogen bond donor competes with the NH group of Cys4 for the carbonyl oxygen atom of Cys1 as hydrogen bond acceptor, plays a relevant role for the structure and spectroscopic properties of the peptide. Since Gly is more exposed to the solvent, its hydrogen-bonding capability can be partially blocked by external solvent molecules in solution or by a second peptide molecule in the crystal. Furthermore, the presence of only one molecule of acetonitrile is sufficient to change the preferred conformation of **1**, and even in acetonitrile solution the simulations suggest that on average only one solvent molecule strongly interacts with the cyclic core of the peptide.

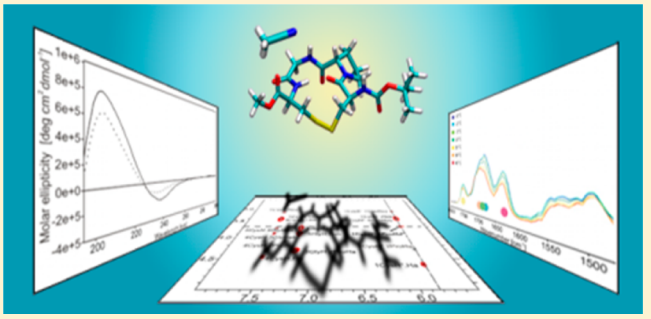

I. INTRODUCTION

Peptides are highly flexible molecules, and in most cases, a large number of rapidly interchanging conformers are found at room temperature. The relative stability of peptide conformers depends on weak intramolecular interactions, in particular hydrogen bonds, but also on angle strain and steric repulsion. Common motifs of the secondary structures of peptides, such as α-helices, β-sheets, and β-turns, are stabilized by these intramolecular interactions. While a quantitative experimental and theoretical description of peptide conformations in the gas phase is already challenging, it becomes even more difficult in solution or in the solid state. In condensed phase the intramolecular interactions that define the secondary structure compete with solvent and other intermolecular interactions. Solvents can act both as hydrogen donors and acceptors and interrupt intramolecular hydrogen bonds by blocking donor or acceptor sites of the peptide. This, in turn, will change the conformer distribution by changing the relative stability of conformers. The picture becomes even more complex if the dynamics of a peptide is taken into account. Treating conformers as static minima on a potential energy surface is an oversimplification that omits most of the conformational space that characterizes a peptide.

The conformational analysis of small peptides in solution is also challenging because of their high flexibility and frequent lack of well-defined structures. Experimental and computational studies of peptides with diverse structural motifs are described in the literature.[1−10] Cyclization reduces the number of possible conformers, and conformational studies of several cyclic pseudohexapeptides and of tetrapeptides were reported.[11−14] Perczel et al.[11] observed that the pseudohexapeptide cyclo(Gly-Pro-Ser(OtBu)-Gly-(δ)Ava) exhibits an "ideal" β-I turn

Received: January 22, 2013
Revised: March 5, 2013

   dx.doi.org/10.1021/jp4007334 | J. Phys. Chem. B XXXX, XXX, XXX−XXX

conformation in the solid state, whereas in solution the presence of two or more conformers was detected. The conformational properties of a small number of cyclic pseudohexapeptides were investigated in several solvents using IR spectroscopy.[15] Five cyclic Pro-X tetrapeptides cyclo(Boc-Cys-Pro-X-Cys-NHMe) (X = Aib, L-Ala, D-Ala, Gly, and L-Leu) were studied by NMR and CD spectroscopy.[16] In solution, all Pro-X tetrapeptides—except for Pro-Aib—preferably adopt distinct β-turns depending on the incorporated Pro-X sequence. A 3_{10} helical conformation (type III β-turn) of the cyclic tetrapeptide cyclo(Boc-Cys-Pro-Aib-Cys-NHMe) involving two intramolecular hydrogen bonds (4 →1) was identified in the solid state.[13] In contrast, a type II β-turn structure of Pro-Aib disulfide is favored in $CDCl_3$, whereas in DMSO-d_6 two different β-turns (II and III) can be found. Falcomer et al.[12] synthesized six tetrapeptides cyclo(Ac-Cys-Pro-X-NHMe) (X = Gly, Phe, Asn, Val, and Ser) and used X-ray crystallography and NMR spectroscopy to characterize the cyclo(Ac-Cys-Pro-Val-NHMe) and cyclo(Ac-Cys-Pro-Ser-NHMe) peptides.

Experimental studies of the effect of solvent and temperature on the conformation of small peptides are much less frequent. *N*-Methylacetamide (NMA) has been intensively investigated both theoretically and experimentally as a simple model of the peptide linkage.[17−22] NMA can also serve as a model for solvent-exposed peptides, as demonstrated by Kubelka et al.[23] The temperature dependence of the amide I vibrational frequency of NMA was studied in several solvents.[24]

Here, we introduce the cyclic disulfide-bridged tetrapeptide cyclo(Boc-Cys1-Pro-Gly-Cys4-OMe) (**1**) and investigate in detail its conformational properties using X-ray crystallography, two-dimensional NMR spectroscopy, temperature-dependent ^{1}H NMR and IR spectroscopy, and UV−CD spectroscopy in combination with molecular dynamics simulations (MD) and quantum mechanics (QM) calculations. Peptide **1** was selected since the cyclic structure restricts the conformational space, and the peptide is small enough for a detailed spectroscopic and computational analysis. In particular, the amide I region of the peptide is relatively simple with few overlapping bands, which allowed us to assign all carbonyl groups in the molecule. In addition, we chose peptide **1** due to its similarity to cyclo(Boc-Cys-Pro-Aib-Cys-OMe) (**2**), for which the ultrafast hydrogen bond dynamics was studied by transient two-dimensional IR spectroscopy.[25] For **2** it was shown that in acetonitrile it adopts a β-turn structure that, even after breaking the disulfide bridge, persists for more than 200 ps. Furthermore, an exceptionally long lifetime of the cysteinyl radicals generated after the photocleavage of the disulfide bond of **2** was measured. The mechanism of photocleavage, unfolding dynamics, and recombination of the cysteinyl radicals of **2** was investigated using multiscale simulations in vacuum and solution.[26]

Peptide **1**, with Aib substituted by Gly, is conformationally more flexible than **2** and thus an interesting molecule to study the influence of solvent and temperature on the conformation. Since the various conformers of **1** are energetically close to each other, temperature-dependent studies are in particular useful to obtain information about their relative stability. Variation of the solvent or the absence of a solvent in the gas phase and in the solid state also changes the conformer population. The combination of all these data allows us to draw an unprecedentedly detailed picture of the solvent- and temperature-driven conformational changes in the model peptide **1**.

II. MODEL AND METHODS

A. Single-Crystal Structure Determination. A single crystal of **1** was grown from hexane−ethyl acetate for X-ray diffraction analysis. The X-ray intensity data for **1** were measured in the ω scan mode on an Oxford Diffraction Xcalibur2 diffractometer with a Sapphire2 CCD, using graphite-monochromatised Mo K_α radiation. The data were processed with CrysAlisPro.[27] A semiempirical absorption correction based on multiple-scanned reflections was applied.[28] The crystal structure was solved by direct methods with SHELXS-97 and refined by full-matrix least-squares refinement on F^2 using SHELXL-97.[29] The absolute configuration was assigned from the known configuration of the starting material and confirmed by a Flack x parameter of 0.00(6).[30] Anisotropic displacement parameters were introduced for all non-hydrogen atoms. Hydrogen atoms were placed at geometrically calculated positions (NH, 0.88 Å; CH, 1.00 Å; CH_2, 0.99 Å; CH_3, 0.98 Å) and refined with the appropriate riding model and $U_{iso}(H) = 1.2U_{eq}(C,N)$ (1.5 for methyl groups). The initial torsion angles of the methyl groups were determined via difference Fourier syntheses and refined while the tetrahedral geometry was held. Crystal data and refinement details are given in Table S1 (Supporting Information). The crystal structure is provided as a supplementary file (see Supporting Information).

B. Temperature-Dependent FITR/ATR Spectra. Peptide solutions were transferred with a syringe into a thermostabilized flow through top-plate assembly with a ZnSe 45° crystal (six reflections, 550 μL sample volume, temperature range −10 to 90 °C; Specac), which was connected to a ATR optics unit (Specac Gateway ATR system). The ATR optics unit was placed in the sample compartment of the FTIR spectrometer (a Bruker IFS66v/S, Bruker Optics). The thermostabilized top-plate was connected to a thermostat (Haake Fison CH) to achieve temperature control. An electronic temperature sensor (Voltcraft 300 K digital thermometer, Conrad Electronics) was used to check the temperature near the ZnSe crystal. All measurements were carried out with 4 cm^{-1} resolution in the spectral range between 400 and 3000 cm^{-1}.[14]

C. NOESY Spectra. The samples of **1** were prepared in DMSO-d_6 or CD_3CN for NMR spectroscopy. The concentration of **1** was adjusted to 4.9 mM. The 1D ^{1}H NMR spectra were recorded at 303 K with a time domain of 32 k data points, mixing times set to 300 ms, and a spectral width of 12019.23 Hz. The sweep width of the 2D homonuclear spectra for **1** in DMSO-d_6 was 4084.97 Hz in the direct and indirect ^{1}H-dimensions. The free-induction decay was acquired for 200.00 ms with a dwell time set to 122.40 μs. For **1** in CD_3CN spectral width of 3019.32 Hz was chosen. The free-induction decay was acquired for 191.28 ms with a dwell time set to 165.60 μs. All spectra were zero-filled prior to Fourier transformation, and sine apodization functions were applied in both dimensions. All spectra were processed with NMR-Pipe.[31] Assignment and data handling were performed using CcpNmr Analysis 2.1.5.[32]

D. NMR Structure Calculations. NOE assignment and structure calculations were performed using CYANA 2.1 and XPLORNIH 2.29.[33−38] NOEs were derived from homonuclear two-dimensional NOESY spectra. All protons were explicitly defined in the dynamically simulated annealing calculations; in some cases, however, additional terms were added to the upper bounds as a pseudoatom correction.[33,34] Structure calculations of the peptide **1** in both solvents, DMSO-d_6 and CD_3CN, were

dx.doi.org/10.1021/jp4007334 | J. Phys. Chem. B XXXX, XXX, XXX−XXX

performed using standard slow cooling protocols for simulated annealing constraint methods implemented in the program XPLOR-NIH and as previously published.[34,39] Structures were validated using PROCHECK and compared according to average RMSD values for C_α, C′, and N atoms. Structure visualization and superpositions were carried out using PyMol.[40]

Compound **1** in DMSO-d_6 was calculated on the basis of 43 NOEs, of which 39 are short-range ($|i - j| \leq 1$ amino acid residue) and one is medium-range ($1 < |i - j| < 5$) NOEs. This corresponds to an average of 10.75 NOEs per amino acid of the peptide sequence. The structure of **1** in CD_3CN was calculated from a total of 39 NOEs, which are divided into 38 short-range ($|i - j| \leq 1$ amino acid residue) and one medium-range ($1 < |i - j| < 5$) NOE, yielding an average of 9.75 NOEs per amino acid of the peptide sequence.

E. UV−CD Spectra. CD spectra of **1** were recorded on a JASCO J-815 spectropolarimeter by using 0.1 cm path length cells at temperatures from 20 to 60 °C. Spectra were recorded at peptide concentrations of ∼0.1 mg/mL. CD data are expressed as molar ellipticity (deg cm^2 $dmol^{-1}$).

F. Computational Details. The cyclo(Boc-Cys1-Pro-Gly-Cys4-OMe) peptide was calculated in the gas phase, water, and acetonitrile at 300 K using the GROMACS program.[41−44] For the simulations in solvent, the peptide was placed in a water or acetonitrile box (water box, 4.047 nm size, 2152 water molecules, spc216 water model;[45] acetonitrile box, 4.260 nm size, 937 acetonitrile molecules, 3 sites acetonitrile model).[46] *NPT* and *NVT* simulations (Berendsen thermostat and barostat) of 100 ps with a time step of 1 fs were performed in all cases to ensure that the system pressure did not change radically in each case. Subsequently, an initial production MD of 500 ps with 1 fs time step (Nosé−Hoover thermostat) was run for each system. These results were used for analyzing the effect of the solvent (peptide in gas phase, water, and acetonitrile at 300 K). For the system in acetonitrile, additional 500 ps of MD simulations were performed with a smaller time step of 0.5 fs. To investigate the effect of the temperature, additional MD simulations at 200, 250, 350, and 400 K were also performed following the same methodology.

A slightly larger acetonitrile box (940 molecules, 4.430 nm) was used (after the *NPT* and *NVT* equilibration steps described above) for a 1 ns production molecular dynamics simulation at 300 K in which the peptide distance restraints from NMR experiments were simulated in a time-dependent approach.[47] For the comparison between the results from this MD simulation and the experimental data, the average distance for two atoms restraints was considered. For more than two atoms restraints, e.g. the restraints between the *tert*-butyl group and the α hydrogen atom of the next amino acid, pair distribution functions ($g(r)$) were used for a better representation of the simultaneous interaction of the nine hydrogen atoms of the *tert*-butyl group and the single α hydrogen atom. The OPLS force field was used in all MD simulations.[48,49]

For the simulation of the spectra, Car−Parrinello molecular dynamics simulations of the tetrapeptide in acetonitrile were carried out using the CPMD package.[50,51] A quasi-infinite solution phase was described by applying periodic boundary conditions to a cubic unit cell of length 22 Å containing the peptide and 55 acetonitrile molecules. Solute and solvent were treated on an equal footing using density functional theory with the PBE functional[52,53] and a plane wave basis set truncated at 25 Ry in conjunction with ultrasoft pseudopotentials.[54] The coupled equation of motion for electronic and nuclear degrees of freedom were solved with a time step of 10 au having replaced all hydrogen atoms by deuterium and set the fictitious electron mass to 1000 au. For each temperature, a production run of ca. 12 ps length was performed following equilibration. The simulations were carried out in the canonical ensemble using a Nosé−Hoover chain thermostat with a coupling frequency of 4000 cm^{-1}.

Vibrational density of states spectra were calculated from the velocity−velocity autocorrelation functions by Fourier transform. The contributions from each carbonyl group were analyzed separately by selecting the corresponding C and O velocities. The frequencies were subsequently rescaled to correct for the damping of nuclear motion due to the fictitious Car−Parrinello electron dynamics. The scaling factors were chosen such as to align the theoretical OMe peak with respect to experiment, yielding values of 1.0828 and 1.0943 at 300 and 400 K, respectively.

Eleven representative snapshots from the simulations in acetonitrile were used as starting point for QM optimizations of the peptide and one molecule of acetonitrile (the calculations were performed at the M05-2X/6-31+G(d,p)[55,56] level of theory using the Gaussian 09 Revision B.01 suite of programs).[57] For the peptide in the gas phase, eight snapshots from the MD simulations were optimized at the same level of theory.

III. RESULTS

The cyclo(Boc-Cys-Pro-Gly-Cys-OMe) peptide (**1**), as well as the other peptides described here, were prepared following a synthesis plan adapted from a peptide synthesis strategy previously published by us[14] (pp S14−S18, Supporting Information). The structural properties of **1** in the solid state and in solution, as well as the effect of temperature and solvent on peptide folding, were investigated using X-ray crystallography together with spectroscopic and computational techniques.

A. Peptide 1 in the Solid State, X-ray Crystallography. The three-dimensional structure and the backbone conformation of peptide **1** in the solid state were investigated by X-ray crystallography. Peptide **1** crystallizes in the monoclinic space group $P2_1$ (Figures 1 and S1 and Table S1, Supporting Information). The comparison of the dihedral angles with the literature shows that peptide **1** features a β-II turn in the solid state (Table S2, Supporting Information).[58]

The 5.3 Å distance between C11 and C15 is also in agreement with a β-turn structure, since according to the general definition of a β-turn by Lewis et al.[59] the distance between αCi and αC(i+3) should be less than 7 Å. The β-II turn in **1** is stabilized by the $C{=}O_{Cys1}{\cdots}H{-}N_{Cys4}$ hydrogen bond at a H···O distance of 2.4 Å (the N···O distance is 3.2 Å, and the N−H−O angle is 144°). These values are close to those reported for hydrogen bonds in other peptides.[60] However, it is known that the presence of an intramolecular hydrogen bond is not mandatory for a β-turn structure.[61] This is confirmed by MD simulations of **1** in the gas phase and solution. The MD simulations reveal that, although the majority of the cyclo(Boc-Cys-Pro-Gly-Cys-OMe) conformers feature a Cys−Cys hydrogen bond in solution, a less compact conformer is preferred in the gas phase (vide infra).

In addition to intramolecular interactions described above, intermolecular interactions are also found in the crystal of **1**: the Gly amide hydrogen atom (see N3 nitrogen, Figure 1,

dx.doi.org/10.1021/jp4007334 | J. Phys. Chem. B XXXX, XXX, XXX−XXX

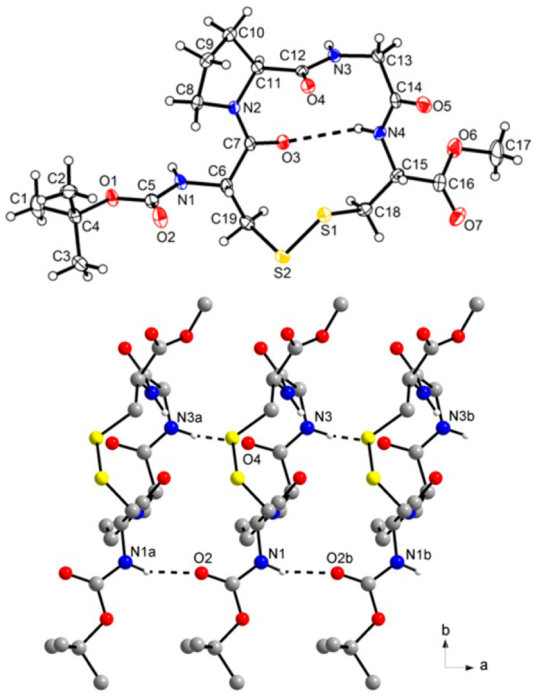

Figure 1. Top: Molecular structure of **1** in the crystal. Displacement ellipsoids are drawn at the 50% probability level. Hydrogen atoms are represented by small spheres of arbitrary radii. The intramolecular N−H···O hydrogen bond is illustrated by a dashed line. Bottom: Intermolecular N−H···O hydrogen bonds (dashed lines) of **1** in the crystal. Carbon-bound hydrogen atoms are omitted for clarity. Symmetry codes: (a) −1 + *x*, *y*, *z* and (b) 1 + *x*, *y*, *z*.

bottom) forms a hydrogen bond with the carbonyl oxygen of the Pro residue of another molecule of **1**, while the Cys1 amide hydrogen (see N1 nitrogen atom in Figure 1, bottom) interacts with the Boc carbonyl oxygen of the neighbor peptide molecule. Because the amide group of Cys1 is not involved in intramolecular interactions, it is not utterly relevant for the peptide conformational behavior. In contrast, the Gly residue considerably influences conformer's distribution in **1**. Remarkably, an analogous behavior to the solid state is found for **1** in solution: the MD simulations of **1** in acetonitrile show that both amide hydrogen atoms of Gly and Cys1 are engaged in interactions with the solvent (see Supplementary Movie, Supporting Information). The intramolecular hydrogen bond as well as the intermolecular interactions in the crystal of **1** are characteristic for cyclic peptides.[62,63]

B. Comparison with Crystal Structures of Other Cyclic Peptides. Only few crystal structures of cyclic tetrapeptides are known. Thus, it is instructive to compare the structure of **1** to the published crystal structures of the similar cyclic peptides cyclo(Boc-Cys-Pro-Aib-Cys-NHMe) (**3**), cyclo(Ac-Cys-Pro-Ser-Cys-NHMe) (**4**), and cyclo(Ac-Cys-Pro-Val-Cys-NHMe) (**5**)[12,13] (Figure 2 and Table S3, Supporting Information).

In the solid state, **3** exhibits two hydrogen bonds, one analogous to that in **1** between the cysteine residues ($C{=}O_{Cys1}{\cdots}HN_{Cys4}$ distance is 2.5 Å, the corresponding O···N distance 2.9 Å, and the H−N−O angle is 13°). The other hydrogen bond is found between the carbonyl group of proline ($C{=}O_{Pro}$) and the NH group of NHMe (N···O is 3.0 Å; H−N−O is 13°). The presence of these two hydrogen bonds results in the compact 3_{10} helix structure (also known as β-III turn) of **3** (φ_{Pro2} = −61°, ψ_{Pro2} = −35°, φ_{Aib} = −61°, ψ_{Aib} = −18°). Both cyclic tetrapeptides **1** and **3** crystallize with the energetically favored *trans*-Cys-Pro peptide bond. The disulfide bridge of **3** is right-handed with a dihedral angle C−S−S−C (χ_{ss}) of 82°, while **1** is left-handed with a dihedral angle of −82°. Since these values are very close to the ideal dihedral angle of 90° for a disulfide bridge, both peptides can be considered almost strain-free. In addition, the endocyclic dihedral angles of the pyrrolidine ring of **1** and **3** are similar, and both show a C_γ-endo conformation. All peptide bonds are nearly planar; bond lengths and angles deviate barely from the standard values. In addition to the two intramolecular hydrogen bonds, the crystal packing of **3** shows a hydrogen bond between the Aib amide hydrogen atom NH and one solvent molecule of DMSO (N···O = 2.9 Å, H−N−O = 19°). In contrast, in peptide **1** the Gly amide hydrogen atom is associated with the oxygen atom of the $C{=}O_{Pro}$ group of another molecule of **1** (Figure 1, bottom).

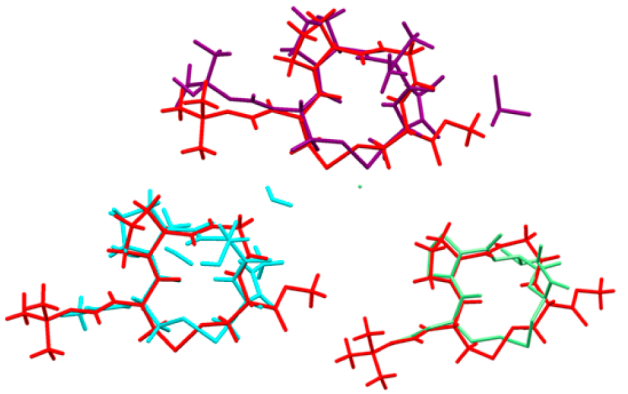

Figure 2. Cyclo(Boc-Cys-Pro-Gly-Cys-OMe) (**1**) (red) in comparison with (top) cyclo(Boc-Cys-Pro-Aib-Cys-NHMe) (**3**, magenta), (bottom left) cyclo(Ac-Cys-Pro-Ser-Cys-NHMe) (**4**, cyan), and (bottom right) cyclo(Ac-Cys-Pro-Val-Cys-NHMe) (**5**, green).[12]

Cyclo(Ac-Cys-Pro-Ser-Cys-NHMe) (**4**) and cyclo(Ac-Cys-Pro-Val-Cys-NHMe) (**5**) both exhibit a *trans*-Cys-Pro peptide bond and an $C{=}O_{Cys1}{\cdots}NH_{Cys4}$ intramolecular hydrogen bond [N···O = 3.1 Å, H−N−O = 22° (**4**); N···O = 3.0 Å (**5**)], similar to that found in **1**. However, while **1** shows a β-II turn structure in the solid state, the dihedral angles φ and ψ of Cys1 and Pro2 in peptides **4** and **5** indicate a β-I turn structure for both peptides. This is in accordance with the results of Kolaskar et al., showing that Pro-Gly segments prefer a β-II turn structure, while the other Pro-X segments mostly adopt β-I turn structures.[64] Peptide **4** shows an additional intermolecular H-bond between the amide proton of serine (NH_{Ser}) and a water molecule. The oxygen atom of the same water molecule is forming a further H-bond with the hydroxyl hydrogen atom of serine (OH_{Ser}). A weak interaction is found between the amide proton NH_{Cys1} and the oxygen of $C{=}O_{Ser}$ of another peptide molecule of **4**.[12] In addition to the backbone $C{=}O_{Cys1}{\cdots}NH_{Cys4}$ hydrogen bond in peptide **5**, the amide hydrogen atom NH_{Cys1} is forming an intermolecular hydrogen bond with $C{=}O_{NHMe}$ of another peptide molecule of **5**. Unlike the amide hydrogen NH_{Ser} of **4**, NH_{Val} of **5** is not associated with a solvent molecule. The methylamide NH groups of both peptides are apparently not involved in interactions with other solvent molecules in the solid state.[12]

The C−S−S−C dihedral angles in peptides **4** (70°, right-handed S−S) and **5** (−77°, left-handed S−S) strongly deviate from the ideal angles (+90° or −90°) of disulfide bridges. This

dx.doi.org/10.1021/jp4007334 | J. Phys. Chem. B XXXX, XXX, XXX−XXX

indicates strain in the disulfide bridges, which results in a destabilization of the peptides. Both peptides crystallize in the same space group $P2_12_12_1$ as **3**, whereas the endocyclic dihedral angles of the pyrrolidine ring with a C_γ-exo conformation are different from those of **3**.

C. Conformers of Peptide 1, Molecular Dynamics (MD) Simulations. To investigate the conformational flexibility of peptide **1**, we performed molecular dynamics simulations under different solvation and temperature conditions. The H bond between the cysteine residues is used here as an indicator of how tight the conformation adopted by the peptide is. Taking as a reference the Cys1−Cys4 hydrogen bond distance ($C{=}O_{Cys1}{\cdots}NH_{Cys4}$) in the peptide crystal structure, we define four groups of conformers: **A**, with the Cys1−Cys4 hydrogen bond distance taking values between 4.0 and 3.0 Å; **B** (crystal structure-like), with a hydrogen bond distance between 3 and 2.2 Å; and **C** and **D**, in which the Cys1−Cys4 hydrogen bond distance takes values shorter than 2.2 Å or larger than 4.0 Å, respectively. The unconstrained simulations of **1** at 300 K in acetonitrile are taken as a reference for further comparisons.

Type **B**, with Cys1−Cys4 hydrogen bond distances similar to that of the crystal structure (2.4 Å) is the most populated group at 300 K in acetonitrile (Table 1). Temperature plays an important role in the structural properties of the peptide, and higher temperatures result in a broader distribution of the Cys1−Cys4 hydrogen bond distances. The population of the less favored conformer group **A** with larger Cys1−Cys4 distances increases at higher temperatures (Table 1). Small amounts of the conformer group **D** with even larger Cys1−Cys4 distances appear at 350 K, but the population of **D** remains very low at all temperatures. Thus, as expected, lower temperatures lead to higher structural selectivity and a narrower distribution of conformers.

Table 1. Population of Conformers (%) in Acetonitrile during the Last 300 ps of the MD Simulations

conformer	200 K	250 K	300 K	350 K	400 K
A	5.7	16.1	20.9	31.6	34.7
B	90.4	77.1	75.4	63.1	62
C	3.9	6.8	3.7	5.1	3.1
D	0.0	0.0	0.0	0.2	0.2

In addition to the temperature, the choice of solvent strongly affects the distribution of conformers. The comparison between the Cys1−Cys4, Cys4−Pro, and Cys1−Gly hydrogen bond distances reveals that in the gas phase the Cys1−Gly interaction is preferred over the Cys1−Cys4 hydrogen bond (Table S4, Supporting Information). In acetonitrile, although the Cys1−Gly hydrogen bonding still is playing an important role in the structural arrangement of the peptide, the Cys1−Cys4 hydrogen bond is shorter, which results in cyclic structures that are more compact compared to those in the gas phase.

For a more systematic analysis of the solvent effect on peptide conformation, the populations of the various conformers were calculated in the gas phase, in water, and in acetonitrile (Table S4, Supporting Information). The differences between the populations in the gas phase and in acetonitrile are remarkable. In the gas phase, conformer group **A** with a larger Cys1−Cys4 hydrogen bond is very much preferred, while in acetonitrile **B** is by far more populated. The differences between the gas phase and acetonitrile can be understood in terms of peptide−solvent interactions, which are lacking in the gas phase but are replaced by similar intermolecular interactions between two adjacent peptide molecules in the solid state. The NH group of Gly serves as hydrogen bond donor and in the gas phase the C═O group of Cys1 as acceptor. In acetonitrile, although the Gly···Cys1 distance takes similar values in the different groups of conformers, the NH group of Gly forms a strong NH···N hydrogen bond with a molecule of acetonitrile as acceptor. This leaves the C═O group of Cys1 "free" to form the Cys1−Cys4 hydrogen bond. A similar but less pronounced effect is found when water is used as solvent. In the peptide−acetonitrile system the NH···N hydrogen bond is stronger than the $C{=}O_{Cys1}{\cdots}HN_{Gly}$ hydrogen bond. In water, on the other hand, the alternative $NH_{Gly}{\cdots}O_{water}$ interaction is of similar strength as the intramolecular Cys1−Gly hydrogen bond. In addition, the strong cooperative effects between the water molecules contribute to weaken the peptide−solvent interaction. The water molecules are able to form more hydrogen bonds, which results in a less compact conformation with respect to those in acetonitrile (Table S5, Supporting Information).

D. Peptide 1 in Solution, UV-CD Spectra. A technique frequently employed to investigate peptide conformations is CD spectroscopy.[65] The CD spectrum of **1** in acetonitrile (CH_3CN) shows a positive band at 203 nm, due to the $\pi{\rightarrow}\pi^*$ transition of the peptide amide bond, and a negative broad band at ~230 nm, attributed to the peptide $n{\rightarrow}\pi^*$ transition (Figure 3). The comparison of the measured CD spectrum of **1** with the CD spectra of other peptides calculated by Woody[65] reveals that **1** follows Woody's class B CD pattern, which indicates a β-turn II conformation. This is consistent with our X-ray structure in the solid state. Moreover, the temperature-dependent CD spectra show that the β-turn structure of **1** is stable up to 60 °C. Changing the solvent from weak hydrogen bond acceptor (CH_3CN) to strong hydrogen bond donor

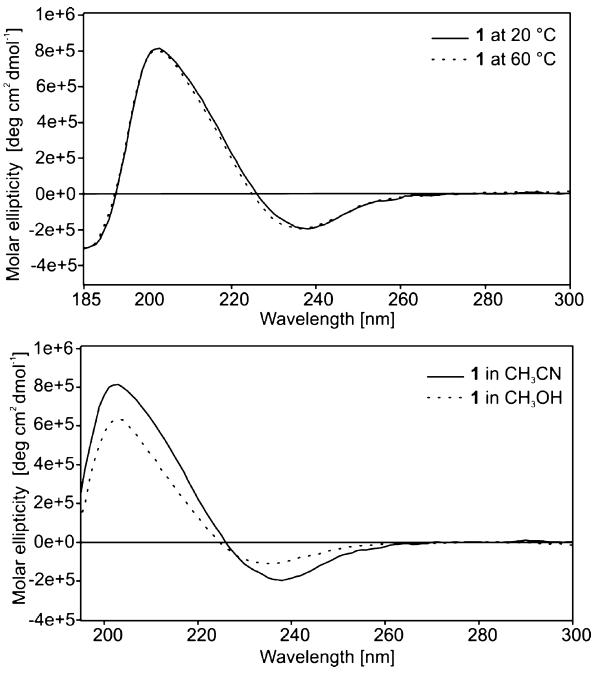

Figure 3. Top: Temperature-dependent CD spectra of **1** in CH_3CN. Bottom: CD spectra of **1** in CH_3OH and in CH_3CN.

dx.doi.org/10.1021/jp4007334 | J. Phys. Chem. B XXXX, XXX, XXX−XXX

(CH_3OH) has no significant effect on the spectrum of **1**, aside from a decrease of the intensity (Figure 3).

E. Peptide 1 in Solution, NMR Experiments. To investigate the conformation of **1** in solution, temperature-dependent ^{1}H NMR experiments were carried out in several solvents. The NMR pattern of **1** in DMSO-d_6 is comparable to that in CD_3CN, indicating a similar distribution of conformers in both solvents (Figure 4).

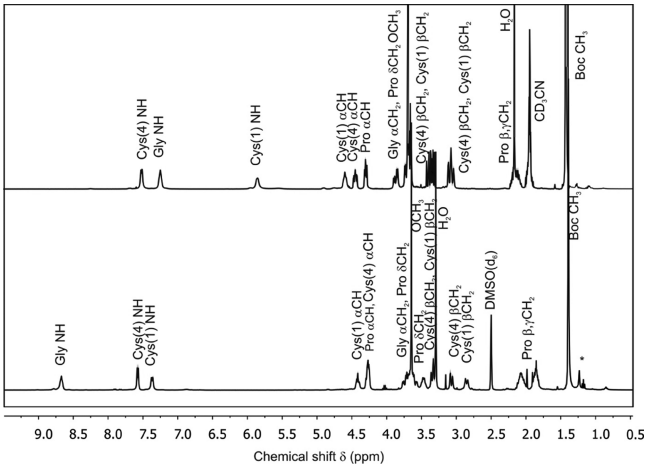

Figure 4. 400 MHz ^{1}H NMR spectra of **1** in (top) CD_3CN and (bottom) DMSO-d_6; the signal marked belongs to ethyl acetate.

For the linear tetrapeptide Boc-Cys(Trt)-Pro-Gly-Cys-(Acm)-OMe (**6**), intramolecular hydrogen bonds are not expected, and indeed the value of $\Delta\delta/\Delta T$ in DMSO-d_6 for all three amide protons is larger than 4×10^{-3} ppm/K, in accordance with the values expected for intermolecular hydrogen bonding (Table 2). In contrast, the temperature

Table 2. Temperature Coefficients of Linear and Cyclic Tetrapeptides in DMSO-d_6 and CD_3CN

compd[a]	Aib NH	L-Phe NH	Acm NH	Gly NH	Cys1 NH	Cys4 NH
$\mathbf{6}_\zeta$	–	–	5.2	5.6	9.2	4.5
$\mathbf{6}_\lambda$	–		4.0	1.8	7.3	3.0
$\mathbf{7}_\zeta$[14]	5.8	–	5.5	–	9.2	2.4
tetra-L-Phe$_\zeta$[14]	–	6.3	5.5	–	9.5	5.2
$\mathbf{1}_\zeta$	–	–	–	4.2	9.0	1.3
$\mathbf{1}_\lambda$	–	–	–	2.4	3.7	1.4
$\mathbf{2}_\zeta$[14]	5.2	–	–	–	9.1	1.7
$\mathbf{2}_\lambda$	3.1	–	–	–	3.5	1.6

[a] ζ, experiments were carried in DMSO-d_6; λ, experiments were carried in CD_3CN.

coefficient of the amide proton of NH_{Cys4} of the cyclic peptide **1** is smaller than 2×10^{-3} ppm/K, indicating an intramolecular H-bond, similar to that observed in cyclo(Boc-Pro-Cys-Aib-Cys-OMe) (**2**).[25] This supports the presence of a C=$O_{Cys1}\cdots HN_{Cys4}$ intramolecular H-bond, in agreement with the MD simulations in acetonitrile and water and similar to what was found in the β-turn II structure of **1** in the solid state.

The temperature coefficients obtained in DMSO-d_6 can be applied to other solvents if the distribution of conformers in these solvents is similar to that in DMSO-d_6.[66] The NMR spectra of peptide **1** in CD_3CN are similar to that in DMSO-d_6, and therefore, changes in the temperature coefficients can be interpreted in a similar manner (Table 2). The comparison of the temperature coefficients in CD_3CN with that in DMSO reveals that in both solvents the major conformer shows an intramolecular hydrogen bond with NH_{Cys4} as donor. Since CD_3CN is a weaker hydrogen bond acceptor than DMSO-d_6, the temperature coefficients in CD_3CN are generally smaller.

F. NOESY Spectra and NMR Structure Calculations. The structures of the cyclic peptide **1** and the linear tetrapeptide **6** in solution were investigated by two-dimensional HMQC-, HMBC-, TOCSY-, and NOESY-NMR spectroscopy. Due to the partial double bond character of the C–N amide bond, a cis–trans isomerization along the peptidyl-prolyl bond occurs on a slow time scale of 10–100 s at 25 °C, which can be directly observed by NMR spectroscopy.[67] Proline-containing peptides show a small energy difference of 0.5–1.4 kcal/mol between the energetically favored trans and cis Xxx-Pro peptidyl-prolyl bond.[67] In small peptides, the amount of cis Xxx-Pro peptidyl-prolyl bonds is increased to 10–30%.[68] The shifts of C_β and C_γ of proline distinguish between cis and trans conformers.[66] The comparison with literature data reveals that peptide **1** adopts exclusively the energetically favored trans Cys-Pro peptidyl-prolyl bond conformation in both DMSO-d_6 and CD_3CN (Table 3).

Table 3. Characteristic ^{13}C Shifts of C_β and C_γ Indicating Cis or Trans Cys-Pro Peptide Bond of Linear and Cyclic Tetrapeptides in DMSO-d_6

peptide	C_β (ppm)	C_γ (ppm)	$\Delta\delta$ ($C_\beta - C_\gamma$) (ppm)
6	28.98	24.38	4.60
1	28.54	24.77	3.77
7	28.52	24.64	3.88
2	28.40	24.85	3.55
trans-Xxx-Pro	29.50[66]	24.20[66]	–
		25.0 ± 1.0[69]	–
		25.1 ± 0.5[69]	1.3–6.0[69]
cis-Xxx-Pro	31.30[66]	22.50[66]	–
		22.4 ± 0.8[69]	–
		23.4 ± 0.3[69]	8.3–10.0[69]

NOEs (nuclear Overhauser effects) arise between two protons that are less than 5 Å apart in space; thus, they provide distance information on pairs of protons.[70] The cross peak of NH_{Cys1} and δCH_{Pro} in the NOESY spectra of **1** evidence the presence of a trans peptidyl-prolyl bond in both solvents (Figure 5).

Furthermore, in peptide **1** the presence of a strong cross peak between NH_{Gly} and NH_{Cys4}, a weaker cross peak of αCH_{Pro} and NH_{Cys4}, and a strong cross peak of NH_{Gly} and αCH_{Pro} support the hypothesis of a β-II turn structure of **1** in solution. Thus, our NOE results are in agreement with the results from temperature-dependent ^{1}H NMR experiments and the X-ray analysis.

In addition, NMR structure calculations were performed to determine the three-dimensional structure of **1** in DMSO-d_6 and CD_3CN (Figure S2, Supporting Information). The ensemble of 20 NMR structures clearly shows the conformational flexibility of the peptide in solution in comparison to the X-ray structure.[71] The NMR ensembles in DMSO-d_6 and CD_3CN are in good agreement with the peptide backbone obtained from the crystal structure.

However, the disulfide bridge and the protecting groups Boc and OMe show, as expected, a higher degree of variation due to

dx.doi.org/10.1021/jp4007334 | J. Phys. Chem. B XXXX, XXX, XXX–XXX

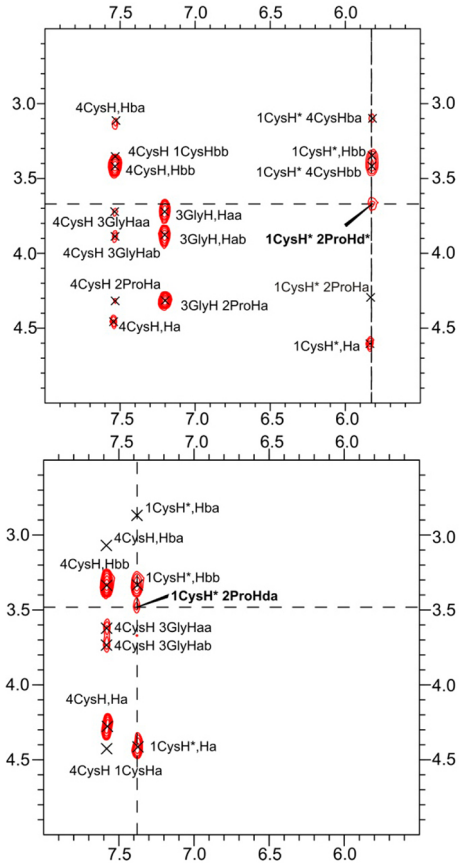

Figure 5. 400 MHz NOESY spectrum showing the $NH_{Cys1}/\delta CH_{Pro}$ cross peaks indicating a trans peptidyl-prolyl bond in (top) CD_3CN and (bottom) DMSO-d_6.

limited NOE contacts. These results are also confirmed by 1 ns MD simulations performed for the restrained peptide in acetonitrile. We found that 21 of the 39 restraints are perfectly within the experimental range, while the other 18 restraints have a certain degree of deviation from the NMR values (Table S6, Figure S3, and more details in Supporting Information). Structural statistics show that in both NMR ensembles no restraint violations occur and that the total energies for the two ensembles are 9.51 and 9.84 kcal/mol, respectively (Table S7, Supporting Information). The RMSD values of the peptide backbone (N, Cα, C′) and the heavy atoms (N, C, O, S) are lower than 0.3 and 0.6 Å, respectively, indicating their high precision. This is in excellent agreement with the RMSD values from the MD simulations that indicate that the RMSD for the backbone is 0.37 ± 0.14 Å and for the heavy atoms is 0.51 ± 0.20 Å (Table S7, Supporting Information).

In both solvents the distances between $\alpha C(i)$ and $\alpha C(i+3)$ of 1 are smaller than 7 Å, indicating a β-turn structure in solution. Furthermore, NMR structure calculations have been performed including a hydrogen bond restraint (O···N = 3 Å, O···H = 2 Å) between $C{=}O_{Cys1}\cdots NH_{Gly(i+2)}$ and $C{=}O_{Cys1}\cdots NH_{Cys4(i+3)}$, respectively. Neither in DMSO-d_6 nor in CD_3CN NOE violations were found. Thus, the experimental NMR restraints support the presence of an intramolecular hydrogen bond (Table S8, Supporting Information).

G. Peptide 1 in Solution, Temperature-Dependent FTIR/ATR Spectra. The IR spectrum of the cyclic peptide **1** in CH_3CN shows distinct absorptions in the amide I region, similar to that of cyclo(Boc-Pro-Cys-Aib-Cys-OMe)[25] **2**, which is used as reference molecule (Figure S4, Supporting Information). Mantsch et al. investigated the IR characteristics of β-turns in different cyclic pseudohexapeptides and attributed the low-frequency absorption of amide I (1645−1630 cm^{-1}) to carbonyl groups involved in intramolecular hydrogen bonding

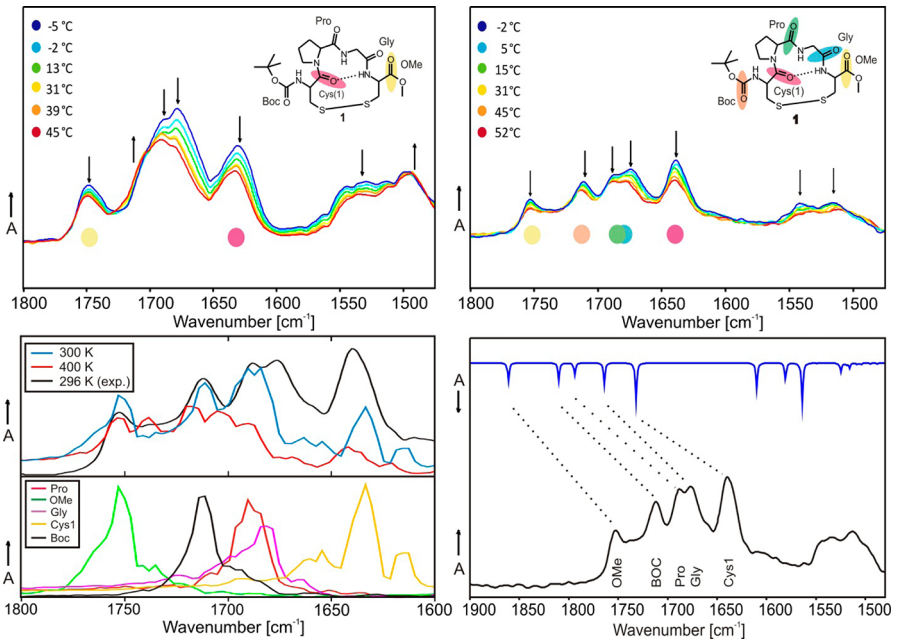

Figure 6. IR characterization of **1**. Top: Static temperature-dependent IR spectra of **1** in $CHCl_3$ (left, 40 mM) and in CH_3CN (right, 20 mM), at a spectral resolution of 4 cm^{-1}. Bottom left: Total theoretical vibrational density of states at 300 K (blue line) and 400 K (red line) from Car−Parrinello MD compared to experimental IR spectrum at 296 K (black line) (upper panel) and theoretical spectra for individual CO groups at 296 K used for the assignment of the peaks (lower panel). Bottom right: Comparison between the calculated spectra of the peptide−acetonitrile complex **acn-I** (blue) and the experimental spectra of the peptide **1** in acetonitrile at 296 K (black).

dx.doi.org/10.1021/jp4007334 | J. Phys. Chem. B XXXX, XXX, XXX−XXX

that stabilize the β-turn (4→1 type).[15] In the cyclic tetrapeptide **1**, the carbonyl band of Cys1 is found in this region, indicating a β-turn stabilized by intramolecular hydrogen bonding between $C{=}O_{Cys1}$ and NH_{Cys4} (Figures 6(top) and S4, Supporting Information). Amide I absorptions in the range between 1680 and 1660 cm^{-1} are most likely carbonyl groups that are not hydrogen bonded and that are sterically constrained.[15] The overlapping carbonyl stretching vibrations of Pro and Gly belong to this group. The remaining two IR bands can be assigned to $C{=}O_{OMe}$, usually appearing at ~1752 cm^{-1}, and to $C{=}O_{Boc}$ (~1711 cm^{-1}). The latter assignment could be confirmed by comparison with studies of Boc deprotection.[72]

In $CHCl_3$, all carbonyl bands—with the exception of OMe—show strong temperature dependence. The overlapping carbonyl bands of Pro, Boc, and Gly (1690−1679 cm^{-1}) rapidly lose intensity on warming the solution and simultaneously undergo a slight blue-shift (Figure 6). The band of $C{=}O_{Cys1}$ at 1631 cm^{-1} decreases in intensity with increasing temperature, although no frequency shift is observed.

Due to the overlapping of three CO oscillators the assignment of the spectra in $CHCl_3$ is difficult. In CH_3CN the CO bands are well separated from each other, and only Pro and Gly are slightly overlapping (Figure 6, top right). Increasing the temperature results in a small loss of intensity, but no significant frequency shift is observed. The $C{=}O_{Cys1}$ band decreases in intensity, but the frequency is not shifted. This is in agreement with the formation of an intramolecular hydrogen bond and evidence that the resulting β-turn structure of **1** is thermally rather stable.

The temperature-dependent FTIR spectra of **1** were compared to Car−Parrinello MD simulations. The simulated vibrational density of states at 300 and 400 K show a good agreement with the experimental spectrum at 296 K (note that the theoretical intensities are not directly comparable to the measured IR absorbances) (Figure 6, bottom left). It is apparent that the spectrum simulated at 400 K shows fewer details than at 300 K, in line with the experimental results. Nevertheless, all peaks are still discernible at 400 K.

A detailed analysis of the MD simulations reveals that in most cases only one molecule of acetonitrile is interacting strongly with the peptide (excluding NH_{Cys1} and the blocking groups OMe and Boc; see Supplementary Movie, Supporting Information). Thus, it is interesting to investigate the structural and spectroscopic properties of the 1:1 peptide−acetonitrile complex. The peptide−acetonitrile interaction involves preferentially the NH group of Gly, although much less frequently an acetonitrile molecule gets close to the NH group of Cys4 (Supplementary Movie, Supporting Information). On this basis, we performed geometry optimizations and calculations of the IR spectra of 11 representative snapshots taken from the MD simulation, considering only the peptide and one molecule of acetonitrile. Interesting enough, most of them converged to the same minimum structure (**acn-I**) and a few to a transition state structure (**acn-II**) with a very low imaginary vibration (5 cm^{-1}) (Figure 7).

In both cases, the acetonitrile molecule is interacting with the NH group of Gly (at 2.2 and 2.1 Å, respectively). However, in **acn-I** two hydrogen atoms of the methyl moiety of acetonitrile weakly interact at about 2.5 Å with oxygen atoms of the carbonyl groups located outside the peptide cycle and corresponding to Cys4 and Gly. The $N_{acetonitrile}{\cdots}HN_{Cys4}$ distance of 3.7 Å is large enough to prevent the acetonitrile

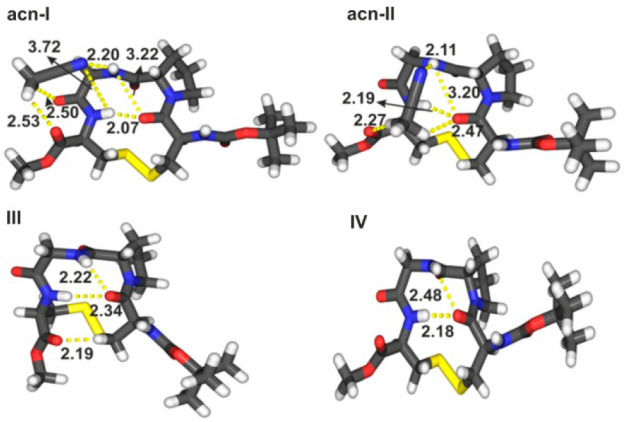

Figure 7. Representative optimized structures of the cyclo(Boc-Cys1-Pro-Gly-Cys4-OMe) peptide **1**: (top) interacting with one molecule of acetonitrile, (bottom) in the gas phase.

molecule from weakening the $C{=}O_{Cys1}{\cdots}NH_{Cys4}$ hydrogen bond at about 2.1 Å. Since the acetonitrile molecule is keeping the NH group of Gly engaged in the $N_{acetonitrile}{\cdots}HN_{Gly}$ interaction, Gly cannot compete with the NH group of Cys4 in forming a hydrogen bond with $C{=}O_{Cys1}$. A similar effect is present in **acn-II**. However, in this structure the position adopted by the acetonitrile molecule results in closer interactions with carbonyl groups of the peptide. The $C{-}H_{acetonitrile}{\cdots}O{=}C_{Cys4}$ interaction takes place now at 2.3 Å while the other hydrogen atom of acetonitrile interacts with the $C{=}O_{Cys1}$ at 2.5 Å. Thus, the effect of diverting the NH group of Gly from interacting with the $C{=}O_{Cys1}$ is additionally preserved by engaging the latter in a weak but non-negligible molecular interaction. On the other hand, this interaction somehow contributes to weaken the Cys1-Cys4 intramolecular hydrogen bond in **acn-II**, resulting in a $C{=}O_{Cys1}{\cdots}NH_{Cys4}$ hydrogen bond distance about 0.1 Å larger than in **acn-I**.

For a complete understanding of peptide folding in **1**, an analysis of the structures in the gas phase is required. The optimizations of eight snapshots of the peptide in the gas phase allowed us to identify the two minima, **III** and **IV** (Figure 7, bottom). **III** is 3.7 kcal/mol more stable than **IV**. The difference in the stabilities of **III** and **IV** is related to the more compact structure of **III**. In this structure the carbonyl group of Cys4 is also interacting with one α hydrogen atom of Cys1 at 2.2 Å. In acetonitrile, the intermolecular interaction with the solvent is stronger, and therefore the intramolecular interaction is not observed in most cases. It is also noticeable how, in the absence of the solvent, the NH group of Gly effectively competes with the NH group of Cys4 for forming a hydrogen bond with the $C{=}O_{Cys1}$ (Figure 7, structure **III**). These calculations, both in the gas phase and in the presence of acetonitrile, also evidence the important role of the weak $C{-}H_{acetonitrile(peptide)}{\cdots}O{=}C_{peptide}$ interaction in determining the structure of the peptide.

The calculated IR spectrum of **acn-I** is in excellent agreement with the experimental spectra (Figure 6, bottom right). This supports the hypothesis that the 1:1 interaction with the solvent largely determines the folding of peptide **1** in acetonitrile. The comparison with the spectra of **III** and **IV** in the gas phase evidences how much the spectroscopic properties depend on the intramolecular H bonding motifs in the peptide (Table 4).

dx.doi.org/10.1021/jp4007334 | J. Phys. Chem. B XXXX, XXX, XXX−XXX

Table 4. Calculated CO Stretching Vibrations (amide I region) for the acn-I, III, and IV Structures (intensities are shown in parentheses)

	C=O stretching				
	OMe	Boc	Pro	Gly	Cys1
acn-I	1861.9 (268)	1810.1 (271)	1794.8 (186)	1764.7 (322)	1732.7 (560)
III	1852.7 (182)	1797.7 (246)[a]	1795.6 (376)[b]	1785.1 (158)[b]	1717.2 (346)
IV	1868.4 (210)	1798.2 (178)	1803.6 (315)[c]	1790.2 (356)	1709.3 (398)

[a]In gas-phase conformer **III**, Boc modes are coupled with Pro and Gly vibrations. [b]Both bands are strongly coupled and cannot be assigned to only one residue. [c]Pro mode appears before Boc and it is coupled with Gly and Boc vibrations.

IV. CONCLUSION

The cyclic disulfide-bridged tetrapeptide cyclo(Boc-Cys-Pro-Gly-Cys-OMe) (**1**) was designed as a model for an in-depth study of solvent-driven conformational changes in peptides. It is highly flexible and small enough to allow both accurate spectroscopy and calculations. It is also one of the few small cyclic peptides that could be characterized by crystal structure analysis. In the crystal, peptide **1** shows a β-turn structure stabilized by a hydrogen bond between Cys1 and Cys4. In the related cyclo(Boc-Cys-Pro-Aib-Cys-OMe) (**2**), this hydrogen bond keeps the β-turn structure in acetonitrile even after rupture of the disulfide bridge for about 200 ps, before evolving into an unfolded structure.[25] Thus, these types of H-bonds define the secondary structure of related peptides in solution. But what is the role of the solvent? MD simulations of **1** suggest that, in general, two major families of conformers, **A** and **B**, can be defined with respect to the Cys1-Cys4 hydrogen bond. Conformer group **A** shows a weak H-bond between Cys1 and Cys4, whereas conformer group **B** shows a stronger hydrogen bond, similar to the structure found in the solid state. The structure of **1** in solution was extensively studied by NMR, UV−CD, and FTIR spectroscopy. These methods are complementary to each other and cover different aspects of the three-dimensional structure and dynamics of **1**. The UV−CD spectra in several solvents give a global picture of the structure and suggest a β-turn II conformation, stable up to 60 °C. This is confirmed by a detailed NMR analysis. The characteristic NMR ^{13}C shifts of the C_β and C_γ atoms of proline show that the peptide adopts exclusively the energetically favored trans conformation of the peptidyl-prolyl bond in DMSO-d_6 and CD_3CN. While NMR spectroscopy presents averaged structures for the rapid conformational interconversions, IR spectra show contributions of all individual conformers present in solution. In combination with Car−Parrinello MD simulations and DFT calculations, the absorptions in the amide I region could be assigned to the individual amino acids. These studies clearly demonstrate the temperature and solvent dependence of the conformer distribution.

Most interesting is that the crystal structure of **1** and the most important structure group **B** both show a strong H-bond between Cys1 and Cys4 at lower temperature in solution. On the other hand, in the gas phase structure group **A** is dominant, and in solution **A** becomes more populated at higher temperatures. The MD simulations suggest that in water at room temperature **B** is also dominant; however, the population of **A**, 27%, is higher than that in acetonitrile, 17% (Table S4, Supporting Information).

The clue to the understanding of the conformer distribution lies in the NH group of Gly, which as hydrogen bond donor competes with the NH group of Cys4 for the carbonyl oxygen atom of Cys1 as hydrogen bond acceptor. Since Gly is more exposed to the solvent, its hydrogen-bonding capability can be partially blocked by external solvent molecules in solution or by a second peptide molecule in the crystal. Thus, in the gas phase Gly has a better chance to form a hydrogen bond to Cys1, which results in conformers of type **A**. Consequently, in acetonitrile the NH group of Gly forms a strong hydrogen bond with a solvent molecule, resulting in a crystal structure-like conformation and the weakening of the Gly-Cys1 interaction with respect to the gas phase. The presence of only one molecule of acetonitrile is sufficient to change the preferred conformation of **1**, and even in acetonitrile solution the simulations suggest that on average only one solvent molecule strongly interacts with the cyclic core of the peptide. Acetonitrile is slightly more efficient than water, since it is a pure hydrogen bond acceptor. The formation of a hydrogen bond with acetonitrile is energetically more favorable than with water, since water is both hydrogen bond donor and acceptor and is thus involved in a network of hydrogen bonds. Besides, our study reveals that the secondary C−H···O=C interactions also play a relevant role on the structural and spectroscopic properties of the peptide. As expected, at higher temperatures the amount of less populated structures increases for a broader conformer's distribution.

■ ASSOCIATED CONTENT

Supporting Information

Peptide synthesis, crystal structure and computational details, and FTIR spectra. This material is available free of charge via the Internet at http://pubs.acs.org.

■ AUTHOR INFORMATION

Corresponding Author

*E-mail: esanchez@kofo.mpg.de (E. S.-G.), wolfram.sander@rub.de (W.S.).

Notes

The authors declare no competing financial interest.

■ ACKNOWLEDGMENTS

C.P. and N.L.D. are grateful for financial support by the Engineering and Physical Sciences Research Council, U.K (EPSRC). E.S-G. acknowledges a Liebig stipend and K.B.-R. a predoctoral stipend, both from the Fonds der Chemischen Industrie, Germany. This work was supported by the Cluster of Excellence RESOLV (EXC 1069) funded by the Deutsche Forschungsgemeinschaft.

■ REFERENCES

(1) Williams, S.; Causgrove, T. P.; Gilmanshin, R.; Fang, K. S.; Callender, R. H.; Woodruff, W. H.; Dyer, R. B. Fast Events in Protein

Folding: Helix Melting and Formation in a Small Peptide. *Biochemistry* **1996**, *35*, 691−697.
(2) Decatur, S. M. Elucidation of Residue-Level Structure and Dynamics of Polypeptides via Isotope-Edited Infrared Spectroscopy. *Acc. Chem. Res.* **2006**, *39*, 169−175.
(3) Montalvo, G.; Waegele, M. M.; Shandler, S.; Gai, F.; DeGrado, W. F. Infrared Signature and Folding Dynamics of a Helical β-Peptide. *J. Am. Chem. Soc.* **2010**, *132*, 5616−5618.
(4) Huang, R.; Setnička, V.;; Etienne, M. A.; Kim, J.; Kubelka, J.; Hammer, R. P.; Keiderling, T. A. Cross-Strand Coupling of a β-Hairpin Peptide Stabilized with an Aib-Gly Turn Studied Using Isotope-Edited IR Spectroscopy. *J. Am. Chem. Soc.* **2007**, *129*, 13592−13603.
(5) Huang, C.-Y.; Klemke, J. W.; Getahun, Z.; DeGrado, W. F.; Gai, F. Temperature-Dependent Helix−Coil Transition of an Alanine Based Peptide. *J. Am. Chem. Soc.* **2001**, *123*, 9235−9238.
(6) Mukherjee, S.; Chowdhury, P.; Gai, F. Infrared Study of the Effect of Hydration on the Amide I Band and Aggregation Properties of Helical Peptides. *J. Phys. Chem. B* **2007**, *111*, 4596−4602.
(7) Kumita, J. R.; Smart, O. S.; Woolley, G. A. Photo-Control of Helix Content in a Short Peptide. *Proc. Natl. Acad. Sci. U. S. A.* **2000**, *97*, 3803−3808.
(8) Ihalainen, J. A.; Bredenbeck, J.; Pfister, R.; Helbing, J.; Chi, L.; Van Stokkum, I. H. M.; Woolley, G. A.; Hamm, P. Folding and Unfolding of a Photoswitchable Peptide from Picoseconds to Microseconds. *Proc. Natl. Acad. Sci. U. S. A.* **2007**, *104*, 5383−5388.
(9) Denschlag, R.; Schreier, W. J.; Rieff, B.; Schrader, T. E.; Koller, F. O.; Moroder, L.; Zinth, W.; Tavan, P. Relaxation Time Prediction for a Light Switchable Peptide by Molecular Dynamics. *Phys. Chem. Chem. Phys.* **2010**, *12*, 6204−6218.
(10) Schreier, W. J.; Aumüller, T.; Haiser, K.; Koller, F. O.; Löweneck, M.; Musiol, H.-J.; Schrader, T. E.; Kiefhaber, T.; Moroder, L.; Zinth, W. Following the Energy Transfer in and out of a Polyproline-Peptide. *Pept. Sci.* **2013**, *100*, 38−50.
(11) Perczel, A.; Hollosi, M.; Foxman, B. M.; Fasman, G. D. Conformational Analysis of Pseudocyclic Hexapeptides Based on Quantitative Circular Dichroism (CD), NOE, and X-ray Data. The Pure CD Spectra of Type I and Type II β-Turns. *J. Am. Chem. Soc.* **1991**, *113*, 9772−9784.
(12) Falcomer, C. M.; Meinwald, Y. C.; Choudhary, I.; Talluri, S.; Milburn, P. J.; Clardy, J.; Scheraga, H. A. Chain Reversals in Model Peptides: Studies of Cystine-Containing Cyclic Peptides. 3. Conformational Free Energies of Cyclization of Tetrapeptides of Sequence Ac-Cys-Pro-X-Cys-NHMe. *J. Am. Chem. Soc.* **1992**, *114*, 4036−4042.
(13) Ravi, A.; Prasad, B. V. V; Balaram, P. Cyclic Peptide Disulfides. Solution and Solid-State Conformation of Boc-Cys-Pro-Aib-Cys-NHMe with a Disulfide Bridge from Cys to Cys, a Disulfide-Bridged Peptide Helix. *J. Am. Chem. Soc.* **1983**, *105*, 105−109.
(14) Kolano, C.; Gomann, K.; Sander, W. Small Cyclic Disulfide Peptides: Synthesis in Preparative Amounts and Characterization by Means of NMR and FT-IR Spectroscopy. *Eur. J. Org. Chem.* **2004**, 4167−4176.
(15) Mantsch, H. H.; Perczel, A.; Hollosi, M.; Fasman, G. D. Characterization of β-Turns in Cyclic Hexapeptides in Solution by Fourier Transform IR Spectroscopy. *Biopolymers* **1993**, *33*, 201−207.
(16) Rao, B. N. N.; Kumar, A.; Balaram, H.; Ravi, A.; Balaram, P. Nuclear Overhauser Effects and Circular Dichroism as Probes of β-Turn Conformations in Acyclic and Cyclic Peptides with Pro-X Sequences. *J. Am. Chem. Soc.* **1983**, *105*, 7423−7428.
(17) Polavarapu, P. L.; Deng, Z.; Ewig, C. S. Vibrational Properties of the Peptide Group: Achiral and Chiral Conformers of *N*-Methylacetamide. *J. Phys. Chem.* **1994**, *98*, 9919−9930.
(18) Mirkin, N. G.; Krimm, S. Ab Initio Vibrational Analysis of Hydrogen-Bonded *trans*- and *cis*-*N*-Methylacetamide. *J. Am. Chem. Soc.* **1991**, *113*, 9742−9747.
(19) Gao, J.; Freindorf, M. Hybrid Ab Initio QM/MM Simulation of *N*-Methylacetamide in Aqueous Solution. *J. Phys. Chem. A* **1997**, *101*, 3182−3188.
(20) Ataka, S.; Takeuchi, H.; Tasumi, M. Infrared Studies of the Less Stable Cis Form of *N*-Methylformmaide and *N*-Methylacetamide in Low-Temperature Nitrogen Matrices and Vibrational Analyses of the Trans and Cis Forms of These Molecules. *J. Mol. Struct.* **1984**, *113*, 147−160.
(21) Mirkin, N. G.; Krimm, S. Conformers of *cis*-*N*-Methylacetamide: Ab Initio Study of Geometries and Vibrational Spectra. *J. Mol. Struct. THEOCHEM* **1991**, *236*, 97−111.
(22) Kubelka, J.; Keiderling, T. A. Ab Initio Calculation of Amide Carbonyl Stretch Vibrational Frequencies in Solution with Modified Basis Sets. 1. *N*-Methyl Acetamide. *J. Phys. Chem. A* **2001**, *105*, 10922−10928.
(23) Kaminský, J.; Bouř, P.; Kubelka, J. Simulations of the Temperature Dependence of Amide I Vibration. *J. Phys. Chem. A* **2011**, *115*, 30−34.
(24) Amunson, K. E.; Kubelka, J. On the Temperature Dependence of Amide I Frequencies of Peptides in Solution. *J. Phys. Chem. B* **2007**, *111*, 9993−9998.
(25) Kolano, C.; Helbing, J.; Kozinski, M.; Sander, W.; Hamm, P. Watching Hydrogen-Bond Dynamics in a Beta-Turn by Transient Two-Dimensional Infrared Spectroscopy. *Nature* **2006**, *444*, 469−472.
(26) Nieber, H.; Hellweg, A.; Doltsinis, N. L. Recyclization Rate of a Photocleaved Peptide from Multiscale Simulation. *J. Am. Chem. Soc.* **2010**, *132*, 1778−1779.
(27) *CrysAlisPro Version 1.171.36.21*, 2012.
(28) Blessing, R. H. An Empirical Correction for Absorption Anisotropy. *Acta Crystallogr. Sect. A* **1995**, *51*, 33−38.
(29) Sheldrick, G. M. A Short History of *SHELX*. *Acta Crystallogr. Sect. A* **2008**, *64*, 112−122.
(30) Flack, H. D. On Enantiomorph-Polarity Estimation. *Acta Crystallogr. Sect. A* **1983**, *39*, 876−881.
(31) Delaglio, F.; Grzesiek, S.; Vuister, G. W.; Zhu, G.; Pfeifer, J.; Bax, A. NMRPipe: A Multidimensional Spectral Processing System Based on UNIX Pipes. *J. Biomol. NMR* **1995**, *6*, 277−293.
(32) Vranken, W. F.; Boucher, W.; Stevens, T. J.; Fogh, R. H.; Pajon, A.; Llinas, M.; Ulrich, E. L.; Markley, J. L.; Ionides, J.; Laue, E. D. The CCPN Data Model for NMR Spectroscopy: Development of a Software Pipeline. *Proteins Struct. Funct. Bioinf.* **2005**, *59*, 687−696.
(33) Brunger, A. T.; Adams, P. D.; Clore, G. M.; DeLano, W. L.; Gros, P.; Grosse-Kunstleve, R. W.; Jiang, J.-S.; Kuszewski, J.; Nilges, M.; Pannu, N. S.; et al. Crystallography & NMR System: A New Software Suite for Macromolecular Structure Determination. *Acta Crystallogr., Sect. A* **1998**, *D54*, 905−921.
(34) Schwieters, C. D.; Kuszewski, J. J.; Clore, G. M. Using Xplor-NIH for NMR Molecular Structure Determination. *Prog. Nucl. Magn. Reson. Spectrosc.* **2006**, *48*, 47−62.
(35) Schwieters, C. D.; Kuszewski, J. J.; Tjandra, N.; Marius Clore, G. The Xplor-NIH NMR Molecular Structure Determination Package. *J. Magn. Reson.* **2003**, *160*, 65−73.
(36) Guntert, P.; Mumenthaler, C.; Wuthrich, K. Torsion Angle Dynamics for NMR Structure Calculation with the New Program DYANA. *J. Mol. Biol.* **1997**, *273*, 283−298.
(37) Herrmann, T.; Güntert, P.; Wüthrich, K. Protein NMR Structure Determination with Automated NOE Assignment Using the New Software CANDID and the Torsion Angle Dynamics Algorithm DYANA. *J. Mol. Biol.* **2002**, *319*, 209−227.
(38) Lopez-Mendez, B.; Guentert, P. Automated Protein Structure Determination from NMR Spectra. *J. Am. Chem. Soc.* **2006**, *128*, 13112−13122.
(39) Stoll, R.; Voelter, W.; Holak, T. A. Conformation of Thymosin B9 in Water/Fluoroalcohol Solution Determined by NMR Spectroscopy. *Biopolymers* **1997**, *41*, 623−634.
(40) *The PyMOL Molecular Graphics System, Version 1.5.0.4*; Schrödinger, LLC.
(41) Hess, B.; Kutzner, C.; van der Spoel, D.; Lindahl, E. GROMACS 4: Algorithms for Highly Efficient, Load-balanced, and Scalable Molecular Simulation. *J. Chem. Theory Comput.* **2008**, *4*, 435−447.

(42) van der Spoel, D.; Lindahl, E.; Hess, B.; Groenhof, G.; Mark, A. E.; Berendsen, H. J. C. GROMACS: Fast, Flexible and Free. *J. Comput. Chem.* **2005**, *26*, 1701−1719.
(43) Lindahl, E.; Hess, B.; van der Spoel, D. GROMACS 3.0: A Package for Molecular Simulation and Trajectory Analysis. *J. Mol. Mod.* **2001**, *7*, 306−317.
(44) Berendsen, H. J. C.; van der Spoel, D.; van Drunen, R. GROMACS: A Message-Passing Parallel Molecular Dynamics Implementation. *Comput. Phys. Commun.* **1995**, *91*, 43−56.
(45) Berendsen, H. J. C.; Postma, J. P. M.; Van Gunsteren, W. F.; Hermans, J. In *Intermolecular Forces*; Pullman, B., Ed.; Reidel Publishing Co.: Dordrecht, 1981; pp 331−342.
(46) Guàrdia, E.; Pinzóna, R.; Casulleras, J.; Orozco, M.; Luque, F. J. Comparison of Different Three-Site Interaction Potentials for Liquid Acetonitrile. *Mol. Simul.* **2001**, *26*, 287−306.
(47) Torda, A. E.; Scheek, R. M.; Van Gunsteren, W. F. Time-Dependent Distance Restraints in Molecular Dynamics Simulations. *Chem. Phys. Lett.* **1989**, *157*, 289−294.
(48) Jorgensen, W. L.; Maxwell, D. S.; Tirado-Rives, J. Development and Testing of the OPLS All-Atom Force Field on Conformational Energetics and Properties of Organic Liquids. *J. Am. Chem. Soc.* **1996**, *118*, 11225−11236.
(49) Kaminski, G. A.; Friesner, R. A.; Tirado-Rives, J.; Jorgensen, W. L. Evaluation and Reparametrization of the OPLS-AA Force Field for Proteins via Comparison with Accurate Quantum Chemical Calculations on Peptide. *J. Phys. Chem. B* **2001**, *105*, 6474−6487.
(50) Marx, D.; Hutter, J. *Ab Initio Molecular Dynamics: Basic Theory and Advanced Methods*; Cambridge University Press: Cambridge, 2009.
(51) CPMD. www.cpmd.org.
(52) Perdew, J. P.; Burke, K.; Ernzerhof, M. Generalized Gradient Approximation Made Simple. *Phys. Rev. Lett.* **1996**, *77*, 3865−3868.
(53) Perdew, J. P.; Burke, K.; Ernzerhof, M. Generalized Gradient Approximation Made Simple [Phys. Rev. Lett. 77, 3865 (1996)]. *Phys. Rev. Lett.* **1997**, *78*, 1396.
(54) Vanderbilt, D. Soft Self-Consistent Pseudopotentials in a Generalized Eigenvalue Formalism. *Phys. Rev. B* **1990**, *41*, 7892−7895.
(55) Zhao, Y.; Schultz, N. E.; Truhlar, D. G. Design of Density Functionals by Combining the Method of Constraint Satisfaction with Parametrization for Thermochemistry, Thermochemical Kinetics, and Noncovalent Interactions. *J. Chem. Theory Comput.* **2006**, *2*, 364−382.
(56) Frisch, M. J.; Pople, J. A.; Binkley, J. S. Self-Consistent Molecular-Orbital Methods. 25. Supplementary Functions for Gaussian-Basis Sets. *J. Chem. Phys.* **1984**, *80*, 3265−3269.
(57) Frisch, M. J.; Trucks, G. W.; Schlegel, H. B.; Scuseria, G. E.; Robb, M. A.; Cheeseman, J. R.; Scalmani, G.; Barone, V.; Mennucci, B.; Petersson, G. A.; et al. *Gaussian 09, Revision B.01*, 2010.
(58) Chou, P. Y.; Fasman, G. D. Beta-Turns in Proteins. *J. Mol. Biol.* **1977**, *115*, 135−175.
(59) Lewis, P. N.; Momany, F. A.; Scheraga, H. A. Folding of Polypeptide Chains in Proteins: A Proposed Mechanism for Folding. *Proc. Natl. Acad. Sci. U. S. A.* **1971**, *68*, 2293−2297.
(60) Stewart, D. E.; Sarkar, A.; Wampler, J. E. Occurrence and Role of Cis Peptide Bonds in Protein Structures. *J. Mol. Biol.* **1990**, *214*, 253−260.
(61) Lewis, P. N.; Momany, F. A.; Scheraga, H. A. Chain Reversals in Proteins. *Biochim. Biophys. Acta* **1973**, *303*, 211−229.
(62) Büttner, F.; Norgren, A. S.; Zhang, S.; Prabpai, S.; Kongsaeree, P.; Arvidsson, P. I. Cyclic β-Tetra- and Pentapeptides: Synthesis Through on-Resin Cyclization and Conformational Studies by X-Ray, NMR and CD Spectroscopy and Theoretical Calculations. *Chem.—Eur. J.* **2005**, *11*, 6145−6158.
(63) Bong, D. T.; Clark, T. D.; Granja, J. R.; Ghadiri, M. R. Self-Assembling Organic Nanotubes. *Angew. Chem., Int. Ed.* **2001**, *40*, 988−1011.
(64) Kolaskar, A. S.; Ramabrahmam, V.; Soman, K. V. Reversals of Polypeptide Chain in Globular Proteins. *Int. J. Pept. Protein Res.* **1980**, *16*, 1−11.
(65) Woody, R. W. *Peptides, Polypeptides & Proteins*; Wiley: New York, 1974; p 338.
(66) Kessler, H. Conformation and Biological Activity of Cyclic Peptides. *Angew. Chem., Int. Ed. Engl.* **1982**, *21*, 512−523.
(67) Fischer, G. Peptidyl-Prolyl Cis/Trans Isomerases and Their Effectors. *Angew. Chem., Int. Ed. Engl.* **1994**, *33*, 1415−1436.
(68) Reimer, U.; Scherer, G.; Drewello, M.; Kruber, S.; Schutkowski, M.; Fischer, G. Side-Chain Effects on Peptidyl-Prolyl Cis/Trans Isomerization. *J. Mol. Biol.* **1998**, *279*, 449−460.
(69) Levy, G. C. *Topics in Carbon-13 NMR Spectroscopy*; Wiley-Interscience, 1976; Vol. *2*.
(70) Brandts, J. F.; Halvorson, H. R.; Brennan, M. Consideration of the Possibility That the Slow Step in Protein Denaturation Reactions Is Due to Cis-trans Isomerism of Proline Residues. *Biochemistry* **1975**, *14*, 4953−4963.
(71) Spronk, C. A. E. M.; Nabuurs, S. B.; Krieger, E.; Vriend, G.; Vuister, G. W. Validation of Protein Structures Derived by NMR Spectroscopy. *Prog. Nucl. Magn. Reson. Spectrosc.* **2004**, *45*, 315−337.
(72) Kolano, C.; Helbing, J.; Bucher, G.; Sander, W.; Hamm, P. Intramolecular Disulfide Bridges as a Phototrigger To Monitor the Dynamics of Small Cyclic Peptides. *J. Phys. Chem. B* **2007**, *111*, 11297−11302.